

Probing molecular associations of field-collected and laboratory-generated SOA with nano-DESI high-resolution mass spectrometry

Rachel E. O'Brien,¹ Tran B. Nguyen,² Alexander Laskin,³ Julia Laskin,⁴ Patrick L. Hayes,^{5,6} Shang Liu,⁷ Jose L. Jimenez,^{5,6} Lynn M. Russell,⁷ Sergey A. Nizkorodov,² and Allen H. Goldstein^{8,9}

Received 25 July 2012; revised 17 October 2012; accepted 11 December 2012.

[1] Aerosol samples from the 2010 CalNex field study in Bakersfield (BF) and Pasadena (LA) were analyzed using positive mode nanospray-desorption electrospray ionization mass spectrometry. Secondary organic aerosol (SOA) produced in a photochemical chamber by photooxidation of diesel (DSL) fuel and isoprene (ISO) under humid, high-NO_x conditions, was analyzed for comparison. Three groups of organic compounds with zero, one, or two nitrogen atoms in their molecular formulas (0N, 1N, 2N) were compared in detail. The composition of ambient SOA exhibited greater overlap with DSL than with ISO. The overlap of the chamber experiments with the BF data was relatively consistent throughout the day while the overlap with LA data increased significantly in the noon to 6 P.M. sample, consistent with the SOA plume arriving from downtown Los Angeles. BF samples were more oxidized, contained more organic nitrogen, and had more overlap with the chamber data compared to LA samples. The addition of gaseous ammonia (NH₃) to the DSL experiment was necessary to generate many of the 2N compounds observed in BF. This analysis demonstrates that DSL and ISO were important sources but cannot account for all of the observed ambient compounds indicating that other sources of organics were also likely important.

Citation: O'Brien R. E., T. B. Nguyen, A. Laskin, J. Laskin, P. L. Hayes, S. Liu, J. L. Jimenez, L. M. Russell, S. A. Nizkorodov, and A. H. Goldstein (2013), Probing molecular associations of field-collected and laboratory-generated SOA with nano-DESI high-resolution mass spectrometry, *J. Geophys. Res. Atmos.*, 118, doi:10.1002/jgrd.50119.

1. Introduction

[2] Organic aerosols (OA), a major fraction of fine (< 2.5 μm) particulate matter, significantly affect visibility, climate, and human health [Charlson *et al.*, 1992; Kanakidou

et al., 2005; Pope and Dockery, 2006; Zhang *et al.*, 2007]. Secondary organic aerosols (SOA), a large fraction of OA, are formed from the gas-to-particle conversion of low-volatility organic compounds, and through aqueous chemistry [Seinfeld and Pankow, 2003; Williams *et al.*, 2010; Ervens *et al.*, 2011]. SOA is a complex mixture resulting from the oxidation of biogenic and anthropogenic organic compounds, and their composition can evolve further through heterogeneous and condensed phase reactions in the atmosphere [Goldstein and Galbally, 2007; Rudich *et al.*, 2007; Donahue *et al.*, 2009].

[3] Although hundreds of organic compounds in SOA have been identified, a large fraction of the organic mass cannot be measured by traditional techniques, e.g., gas chromatography/mass spectrometry (GC/MS), due to the large molecular mass and highly polar nature of many SOA compounds. Soft ionization methods, such as electrospray ionization (ESI) [Fenn *et al.*, 1990], coupled to high resolution mass spectrometry (HR-MS), are well suited for the analysis of these compounds, allowing for the identification of the exact elemental formulas of hundreds to thousands of individual organic molecules in each sample [Tolocka *et al.*, 2004; Reemtsma *et al.*, 2006; Reinhardt *et al.*, 2007; Altieri *et al.*, 2009; Mazzoleni *et al.*, 2010; Nguyen *et al.*, 2010; Schmitt-Kopplin *et al.*, 2010; Hall and Johnston, 2011]. We refer to these molecules as high molecular weight (high-MW) compounds or oligomers. The identities and abundances of observed high-MW species have been demonstrated to change based on the time of year

¹Department of Chemistry, University of California, Berkeley, California, USA.

²Department of Chemistry, University of California, Irvine, California, USA.

³William R. Wiley Environmental and Molecular Sciences Laboratory, Pacific Northwest National Laboratory, Richland, Washington, 99352, USA.

⁴Chemical and Materials Sciences Division, Pacific Northwest National Laboratory, Washington, 99352, USA.

⁵Cooperative Institute for Research in Environmental Sciences (CIRES).

⁶Department of Chemistry and Biochemistry, University of Colorado at Boulder, Boulder, Colorado, USA.

⁷Scripps Institution of Oceanography, University of California, San Diego, La Jolla, California, USA.

⁸Department of Environmental Science, Policy, & Management, University of California, Berkeley, California, 94720, USA.

⁹Department of Civil and Environmental Engineering, University of California, Berkeley, California, 94720, USA.

Corresponding author: A. Laskin, William R. Wiley Environmental and Molecular Sciences Laboratory, Pacific Northwest National Laboratory, Richland, WA 99352, USA. (Alexander.Laskin@pnl.gov) A. H. Goldstein, Department of Civil and Environmental Engineering, University of California, Berkeley, CA 94720, USA. (ahg@berkeley.edu)

[Kalberer et al., 2006] and the impact of intermittent sources such as biomass burning [Schmitt-Kopplin et al., 2010]. Analyzing the chemical composition of high-MW compounds throughout the day can provide additional information on the sources and transformations of the aerosols.

[4] Progress in identifying important chemical reactions and potential sources for high-MW species has been made using smog chamber experiments. The following citations are not meant to be comprehensive, but rather to be illustrative of the range of chamber studies that have been undertaken. Biogenic precursors such as isoprene [Dommen et al., 2006; Nguyen et al., 2011a; Zhang et al., 2011], α -pinene [Gao et al., 2004; Iinuma et al., 2004; Tolocka et al., 2004; Reinhardt et al., 2007], limonene [Walser et al., 2008; Laskin et al., 2010], and anthropogenic precursors, such as 1,3,5-trimethylbenzene [Kalberer et al., 2004; Baltensperger et al., 2005], and cycloalkenes [Gao et al., 2004] have all been found to form high-MW SOA compounds in chamber studies. The mass spectra reported in these studies show differences in the molecular composition of SOA formed from different precursors, and under different experimental conditions. For example, the chemical composition of isoprene SOA changed when it was formed under different relative humidity and NO_x concentrations [Nguyen et al., 2011a; Zhang et al., 2011]. Kalberer et al. compared the composition of ambient SOA to that of chamber SOA generated using different precursors illustrating the potential for comparison studies to provide insights into the sources and chemistry of SOA [Kalberer et al., 2006].

[5] In ESI-MS studies, the aerosol sample is first extracted into an organic solvent and then electrosprayed into the mass spectrometer inlet. Potential solvent-analyte interactions introduced by the extraction step [Bateman et al., 2008] can be alleviated by quick dissolution and ionization of the sample directly from the substrate. A novel technique for this type of analysis is nano-desorption electrospray ionization (nano-DESI) mass spectrometry [Roach et al., 2010b]. Laskin and coworkers have demonstrated the utility of nano-DESI for the soft ionization of complex mixtures on substrates with the potential preservation of some labile species and no sample preparation [Roach et al., 2010a; Eckert et al., 2012].

[6] There have been numerous applications of HR-MS to chamber studies of SOA and the number of field-applications of HR-MS is also growing quickly [Laskin et al., 2012]. However, no systematic studies have been performed on the degree of overlap between molecular level composition of OA collected in the field and OA generated in lab studies. In this work, we present the molecular characterization of organic compounds inferred from nano-DESI/HR-MS analysis of aerosol samples collected in Bakersfield (BF) and Los Angeles (LA) California during the 2010 CalNex campaign. We compare the ambient chemical composition with SOA samples generated in a smog chamber under high NO_x conditions with diesel fuel (DSL) and isoprene (ISO) precursors, and analyzed using the same nano-DESI/HR-MS approach. DSL and ISO SOA were chosen to represent potentially significant anthropogenic and biogenic influences, respectively, at the BF and LA site. Isoprene and diesel are both known sources for SOA [Carlton et al., 2009; Weitkamp et al., 2007]. The nearby vegetation and the prevalence of diesel use near both urban centers suggested that both diesel and isoprene were likely to be important sources at the two field sites. The BF site is also characterized by elevated mixing ratios of ammonia (NH_3)

(M. Z. Markovic et al., Measurements and modeling of water-soluble Q12 composition of $\text{PM}_{2.5}$ and associated precursor gases in Bakersfield, CA during CalNex 2010, *J. Geophys. Res.-Atmos.*, manuscript in preparation, 2012) and additional chamber experiments were performed including the oxidation of DSL in the presence of NH_3 . Hereinafter, the high- NO_x photooxidation of DSL and ISO are referred to as “DSL- NO_x ” and “ISO- NO_x ”, respectively, and the high- NO_x photooxidation of diesel in the presence of NH_3 is referred to as “DSL- NO_x - NH_3 .” Composition differences in the ambient SOA samples throughout the day were inferred from the high resolution mass spectra. The contributions of DSL and ISO to SOA formation BF and LA were investigated and while both were found to be important SOA sources, contributions from other sources, such as gasoline [Bahreini et al., 2012; P. L. Hayes et al., Aerosol Composition and Sources in Los Angeles During the 2010 CalNex Campaign, *J. Geophys. Res.-Atmos.*, submitted manuscript, 2012] and terpenes [Pandis et al., 1991; Griffin et al., 1999], were also indicated.

2. Experimental

2.1. Sampling and Instrumentation

[7] The 2010 CalNex campaign had ground sites in BF and LA as well as aerial and ship-based measurements [National Oceanic and Atmospheric Administration, 2008]. A summary of the field sites, the ambient sampling, and the chamber studies is provided in Section A of the auxiliary material (auxiliary materials are available in the HTML. doi:10.1029/2012JD018558).¹ Briefly, the samples were collected at the BF (35.35°N, 118.97°W) and LA (34.14°N, 118.12°W) sampling sites. 5 June and 23 June were chosen for in-depth analysis, in LA and BF, respectively, because concurrent measurements with an aerosol mass spectrometer (AMS) indicated high SOA loadings on those days (P. L. Hayes et al., submitted manuscript, 2012). For these 2 days the diurnal patterns of the organic fraction from AMS measurements at each site were similar to the average diurnal pattern over the whole campaign. This suggests that these days can be taken as representative of the average trends observed at each site. Samples were collected on aluminum foil substrates using an 8 stage (BF) nonrotating and a 10 stage (LA) rotating Micro-Orifice Uniform Deposit Impactor (MOUDI, MSP Corp.) at ~ 30 standard liters per minute. BF samples were stored in a -20°C freezer at the site and a -80°C freezer at the lab, and LA samples were stored in a -20°C freezer. Samples on the eighth stage of the MOUDI, (size range of 0.18–0.32 μm aerodynamic diameter), showed the largest number of compounds in the MS of the BF samples and were chosen for intensive analysis. For consistency, the same stage was used for the LA samples, which corresponds to the middle of the accumulation mode mass distribution there (P. L. Hayes et al., submitted manuscript, 2012). All times discussed here are in local time (PDT). Online composition of the nonrefractory components of the aerosol was measured using an Aerodyne high-resolution time-of-flight aerosol mass spectrometer (HR-ToF-AMS) at both sites [DeCarlo et al., 2006]. In LA, the size resolved O/C was estimated from HR-ToF-AMS measurements using the relationship $\text{O/C} = 3.25(f_{44}) + 0.001$ where f_{44} is the fraction of the total organic signal at m/z 44 (P. L. Hayes et al., submitted manuscript, 2012). A similar relationship of O/C and f_{44} was found for Bakersfield: $\text{O/C} = 3.02 (f_{44}) + 0.043$

(Figure S1). The conversion between vacuum aerodynamic diameter (D_{va}) and aerodynamic diameter was determined assuming spherical particles and a density of 1.2 g/cm^3 [DeCarlo *et al.*, 2004; Zhang *et al.*, 2005]. For Fourier transform infrared spectroscopy (FTIR) analysis, particles were collected on Teflon filters with 3–6 h time resolution. Concentrations of organic functional groups, including alkane, carboxylic acid, organonitrate groups, etc., were quantified using automated algorithms described previously [Russell *et al.*, 2009; Liu *et al.*, 2011]. Detailed sample collection and organic functional group analysis are presented in Liu *et al.* [2012].

[8] For the chamber experiments, SOA samples were generated from photooxidation reactions in a 5 m^3 Teflon chamber equipped with UV-B broadband lamps in the absence of inorganic seed particles [Nguyen *et al.*, 2011b]. The reaction was carried out at room temperature in the relative humidity range of 60–70%. DSL (diesel # 2 composite standard mixture, Restek, 0.5 g/mL in CH_2Cl_2) or ISO (Aldrich, purity 99%) were injected into the chamber in a clean glass bulb. An estimate of the initial mixing ratios of total DSL organics in the chamber was 100 ppb (assuming an average molecular weight of 230 g/mol [Wilson *et al.*, 1990]) and the initial mixing ratio of ISO was 250 ppb. Nitric oxide (NO, injected from a cylinder containing 5000 ppm in N_2), nitrogen dioxide (NO_2), and ozone (O_3) were introduced into the chamber before the injection of DSL or ISO. The initial mixing ratios were $[\text{NO} + \text{NO}_2 = \text{NO}_x]$: 200–300 ppb and $[\text{O}_3]$: 50–90 ppb. For NH_3 experiments, $\sim 150 \text{ ppb}$ NH_3 (Fluka, 30% in water) was injected with dry air into the chamber before photooxidation. The UV photochemistry of O_3 initiated the photooxidation, similar to conditions in the atmosphere. The photooxidation time was approximately 5 h. The samples were collected through an activated charcoal denuder with a 30 standard liters per minute pump flow rate and humid make-up air onto aluminum substrates using the MOUDI. The collected SOA samples were vacuum sealed and frozen at -20°C for offline high-resolution nano-DESI-MS analyses.

[9] Samples were analyzed at the Environmental Molecular Sciences Laboratory (Richland, Washington). Analysis was performed using a high-resolution LTQ-Orbitrap MS (Thermo Fisher, Bremen, Germany) equipped with a recently developed nano-DESI source [Roach *et al.*, 2010a, 2010b]. The source is assembled from two fused-silica capillaries ($193 \mu\text{m}$ o.d. / $50 \mu\text{m}$ i.d., Polymicro Technologies LLC, Phoenix, AZ). Acetonitrile was injected through the primary capillary forming a small droplet on the analyte surface. The dissolved analyte was transferred into the inlet of mass spectrometer through the nanospray capillary. The solvent was supplied at $1.5\text{--}2.5 \mu\text{L/min}$ flow rate to maintain a stable droplet on the surface. A voltage of $\sim 6 \text{ kV}$ was applied between the capillary end and the mass spectrometer inlet to obtain stable spray of charged droplets, and the system was operated in the positive ion mode with a resolution of $60,000 m/\Delta m$ (FWHM) at m/z 400. Positive mode data were used for this analysis. The instrument was externally mass calibrated using a standard ESI calibration mix of caffeine, MRFA, and Ultramark 1621 (calibration mix MSCAL 5, Sigma-Aldrich, Inc.).

2.2. Data Acquisition/Analysis

[10] Data analysis was performed in a similar manner to our previous work [Nguyen *et al.*, 2011a; Nizkorodov *et al.*, 2011]. Briefly, background mass spectra acquired over

the sample-free area were identified and removed from the mass spectra recorded when the probe was positioned over the sample area with deposited particulate matter [Roach *et al.*, 2010a]. Mass spectral features with a signal-to-noise ratio higher than 3 and a minimum background ratio of 5 were extracted from raw spectra using Decon2LS [Jaitly *et al.*, 2009]. The signal-to-noise ratio was defined as the ratio of the intensity of the peak to the average intensity at the valleys of the peak. The background intensity was defined as the average intensity of the points that are within five standard deviations of the average of all the points in the spectrum. Molecular assignments of the observed ions were performed using MIDAS molecular formula calculator (<http://magnet.fsu.edu/~midas/>) with the following constraints $C \leq 100$, $H \leq 200$, $O \leq 50$, $N \leq 3$, $S \leq 1$, $Na \leq 1$. Approximately 80–90% of the peaks could be assigned molecular formulas and assignments were aided by Kendrick analyses [Kendrick, 1963; Stenson *et al.*, 2003] using O and $\text{C}_3\text{H}_4\text{O}_2$ as base units, and a second-order Kendrick analysis using a sequence of CH_2 and H_2 base units [Roach *et al.*, 2011]. The formula $\text{C}_3\text{H}_4\text{O}_2$ has been found to be a common base unit in atmospheric samples [Altieri *et al.*, 2008; Mazzoleni *et al.*, 2010] and was used here to aid in the identification of molecules that did not fall in families with the other Kendrick base units. No seed particles were used in the chamber studies and no sulfur compounds were observed. Thus, we limit our discussion of the comparisons to $\text{C}_c\text{H}_h\text{O}_o\text{N}_n$ compounds. The mass spectra were acquired over the mass range of m/z 100–1000. However, in this work we limit our discussion to peaks in the 100–400 Da range because they can be unambiguously assigned for $\text{C}_c\text{H}_h\text{O}_o\text{N}_n$ compounds given the mass accuracy and resolution used in this study.

[11] To resolve and identify elemental compositions in complex mixtures such as aerosol, petroleum, and dissolved organic matter samples, both high mass resolution and high mass accuracy are required [Marshall *et al.*, 2006; Reemtsma *et al.*, 2006; Schmitt-Kopplin *et al.*, 2010]. High resolution enables the separation of closely-spaced peaks while high accuracy enables the determination of the elemental composition based on the exact mass. It has been demonstrated through mathematical modeling that $\sim 0.1\text{--}0.5 \text{ mDa}$ mass accuracy is necessary to determine unique elemental composition for typical organic compounds up to 500 Da (and higher when combined with Kendrick analysis) [Marshall *et al.*, 2006]. In an analysis of extracted aerosol filter samples using negative mode ESI, Schmitt-Kopplin and coworkers showed that closely-spaced CHO and CHOS compounds (C_3 vs. SH_4) at $\sim 400 \text{ Da}$ were resolved with an instrument resolution of $\sim 150,000$ [Schmitt-Kopplin *et al.*, 2010]. Compared to their study, we used a relatively lower mass resolution of $60,000 m/\Delta m$ at m/z 400. However, we can still confidently identify peaks over a broad mass range based on the accurate mass measurements. Kendrick analysis aids identification by grouping higher mass peaks into families with lower mass peaks that can be unambiguously identified. The second-order transformation introduced recently [Roach *et al.*, 2011], and used here, enables even more efficient grouping, which facilitates identification of higher-mass peaks within each group that cannot be unambiguously identified using traditional first-order Kendrick analysis. Mass accuracy can be affected by the presence of overlapping, unresolved peaks if the peaks have similar abundance. For

example, an unresolved CHO/CHOS doublet (e.g., $C_{16}H_{28}O_{10}S$ vs. $C_{19}H_{24}O_{10}$) with equivalent abundances would result in an error of ~ 1.7 mDa for either assignment. In contrast, when the relative abundance of one of the peaks in the unresolved doublet is low, the measured mass is very close to the exact mass of the more abundant peak. Under these conditions, while lower abundance species are unresolved and unassigned, the dominant species are accurately identified. In this study the majority (~ 75 – 80%) of our assignments had mass accuracy within ± 0.35 mDa. Some higher mass peaks had both $C_cH_hO_oS_1$ and $C_{c-6}H_{h+1}O_{o+5}Na$ as possible assignments within this mass accuracy. These peaks were assigned as sodiated through the use Kendrick analyses with oxygen and $C_3H_4O_2$ base units. These assignments are consistent with results from *Lin et al.* [2012] showing low numbers of sulfur containing compounds in ambient aerosol samples measured with positive mode ESI. While we do not necessarily resolve all of the peaks in the spectrum, the assignments are accurate as indicated by the absolute error.

[12] The analyte molecules were observed as either protonated ($[M+H]^+$) or sodiated ($[M+Na]^+$) species. The assigned ionic formulas were converted to neutral formulas by subtracting either the exact mass of a proton or a sodium ion. Approximately 0–10% of the compounds in each sample were detected as both sodiated and protonated species. For these peaks, the average intensity was used. In this work, compounds containing zero, one, or two nitrogen atoms (0N, 1N, 2N, respectively) were compared. While analysis focused on positive mode spectra, elemental ratios from analysis of the negative mode spectra were included for comparison with AMS data.

[13] There are many ways to look at the overlap between two measurements. We opted to use the percentage of peaks found in ambient samples that were also found in the chamber studies. The percentage of overlap between the ambient samples and the chamber studies was determined using equation (1).

$$\% \text{ overlap} = \frac{\text{(number of matching peaks)}}{\text{(number of peaks in ambient sample)}} \times 100 \quad (1)$$

where the “matching peaks” are compounds that have the same observed molecular formulas in both the ambient and the chamber study samples. The relative intensities are not included in the overlap calculations due to the variability of ion intensities inherent in ESI. In equation (1) the overlap is divided by the number of peaks in the ambient sample, thus, the relative extent of overlap is not weighted by the number of observed compounds. The number of conceivable molecular formulas of the type $C_cH_hO_oN_n$ that satisfy valence rules and weigh under 400 Da exceeds 10^4 , whereas the number of observed peaks in the field and lab samples was of order 10^3 . The probability of a random match between the samples at the overlap level observed in this work is small. A caveat to this approach is that the chemical formula may correspond to multiple isomers, thus percent overlaps include molecules having the same elemental composition regardless of their structure. This means that a match between two samples does not necessarily indicate that the compound originates from that source. However, a match found for a large fraction of peaks increases the level of confidence in the apportionment. In this study

only the elemental formulas are obtained, however, to aid discussion the terms “molecules” and “compounds” are used here to refer to all the possible isomers with a given molecular formula.

3. Results and Discussion

3.1. Comparing Ambient to Chamber Data

[14] Figure 1 shows a comparison of the high resolution mass spectra from the ambient samples for each location exhibiting the best overlap with DSL- NO_x . The peaks in the mass spectra are color-coded as 0N, 1N, and 2N compounds with molecular formulas $C_cH_hO_o$, $C_cH_hO_oN$, and $C_cH_hO_oN_2$, respectively. Similar comparison mass spectra of all the BF and LA samples with DSL- NO_x , DSL- NO_x - NH_3 , and ISO- NO_x are provided in Figures S2 through S7 in the auxiliary material. The measured peak intensities do not necessarily correlate to the absolute concentrations of the corresponding compounds in the sample. However, larger concentrations generally result in larger relative peak intensities for structurally related compounds, and therefore, qualitative comparison of the peak intensity distributions (overall shapes) in mass spectra is still valuable. The relative intensities were calculated by dividing the measured intensity by the maximum intensity observed in that sample, except where noted. Figure 1a shows that the intensity distributions of the BF sample collected from 6 A.M. to noon and the DSL- NO_x sample were similar, e.g., the maximum intensities occurred over roughly the same mass range and the mass ranges of the

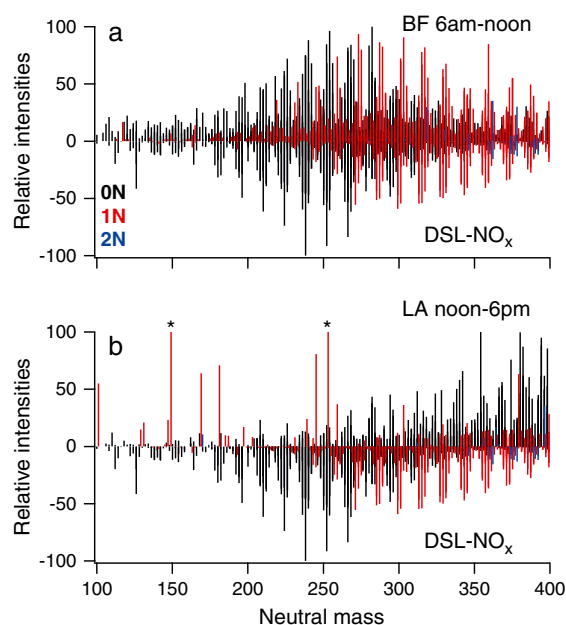


Figure 1. Comparison of the mass spectra of the ambient samples from each site with the best DSL- NO_x overlap: (a) BF 6 A.M. to noon and (b) LA noon to 6 P.M. The DSL- NO_x mass spectra are plotted with negative relative intensities to aid comparison. The colors correspond to the number of N atoms in the chemical formula with black=0N, red=1N, blue=2N. The two starred peaks in the LA noon to 6 P.M. sample have intensities of 260 and 250 on this scale.

different subgroups (0N vs. 1N) correlated reasonably well. In contrast, Figure 1b shows that the LA sample collected from noon to 6 P.M. and the DSL-NO_x sample appeared quite different in terms of the intensity distribution of mass spectral signals. In the LA sample, the intensity distribution was still increasing up to ~400 Da compared to a maximum at ~250 Da for the DSL-NO_x sample. Additionally, there were significantly fewer 1N and 2N compounds compared to the DSL-NO_x sample. A visual comparison of the BF 6 A.M. to noon with the LA noon to 6 P.M. sample (Figures 1a and 1b) shows a dramatically different intensity distribution, likely indicating different source composition/contributions and/or chemistry at the two sites.

[15] Figure 2 shows how the distribution of 0N, 1N, and 2N compounds assigned for each sample changes with the measurement location and time. The total number of compounds in each sample is written above the corresponding column. The BF samples had a relatively consistent number of detected compounds in the night and early morning samples with a decrease in the afternoon (noon to 6 P.M.). In contrast, the LA data had lower numbers of compounds in the night samples and higher numbers of compounds during the day. In all cases, the majority of species were 0N or 1N compounds. The percentage of 2N compounds was below 10% in all samples, and averaged ~4%. The number of 1N or 2N compounds was significantly lower in the LA samples compared to both the BF and the chamber samples.

[16] Figure 3 compares the overlap percentage (equation (1)) of the chamber and ambient sample data. The chamber experiment with the highest percent overlap with BF data was the DSL-NO_x sample (Figure 3a) where 60 to 65% of the compounds identified in the BF sample were also observed in the laboratory SOA. The DSL-NO_x-NH₃ data had the second highest overlap and the ISO-NO_x had the lowest overlap. Within the day in BF, the 6 am to noon sample had the highest percent overlap with the DSL-NO_x and DSL-NO_x-NH₃ samples at 65% and 59%, respectively. The overlap with ISO-NO_x was relatively consistent throughout the day, between 37 and 40%. The BF noon to 6 P.M. sample had the lowest percent overlap with the DSL-NO_x data, even though this sample had the lowest number of

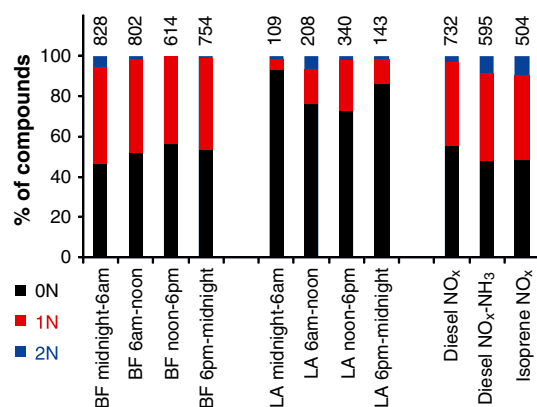


Figure 2. Percentage of formulas assigned 0N, 1N, and 2N for each sample. The 0N, 1N, and 2N compounds correspond to molecular formulas $C_cH_hO_o$, $C_cH_hO_oN$, and $C_cH_hO_oN_2$, respectively. The total number of identified peaks in each sample is shown above each column.

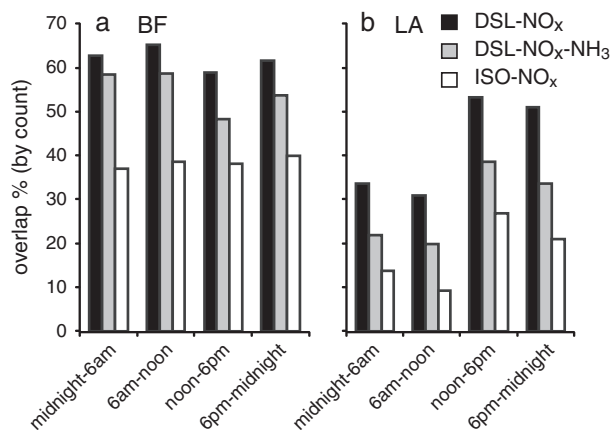


Figure 3. Percent overlap calculated from equation (1) for (a) BF and (b) LA samples with respect to the three chamber studies, DSL-NO_x (black), DSL-NO_x-NH₃ (gray), and ISO-NO_x (white).

identified peaks and thus, would be expected to have the highest overlap if the samples were very similar because in the overlap comparison we divided by the number of peaks in the ambient sample. The total number of overlapping compounds was the lowest for this sample (Table S1), which suggests that either these sources, DSL and ISO, had the least impact on this sample or this sample was affected by different chemistry. Generally, the BF samples showed more overlap with the DSL sample and there were small changes in the overlap with the DSL sample throughout the day. The small changes in overlap could be due to either variations in local sources such as gasoline, diesel, terpenes, etc., or to variations in atmospheric chemistry such as those due to changes in ozone and liquid water content. However, the extent to which variation in either sources or chemistry contributed to the observations cannot be determined from these data. The percent overlap of BF with ISO-NO_x was slightly more constant throughout the day perhaps indicating a more distant, but broadly arrayed, source resulting in a more stable signal, consistent with the high isoprene-emitting oak trees prevalent in the hills surrounding the San Joaquin Valley.

[17] The LA data generally had less overlap with the chamber study data than BF (Figure 3b). The percent overlap between LA and the chamber studies followed the same trend with the highest overlap observed with DSL-NO_x and the lowest overlap observed with ISO-NO_x. The percent overlap varied more within the day in LA, with the DSL-NO_x sample matching ~31% of the compounds from 6 A.M. to noon and ~51% of the compounds from noon to 6 P.M. The much higher percent overlap for the noon to 6 P.M. sample is consistent with the arrival of the afternoon SOA from both DSL and ISO influenced sources. The concentration of elemental carbon and the photochemical age both peaked during the noon to 6 P.M. period also consistent with SOA influenced by DSL sources (P. L. Hayes et al., submitted manuscript, 2012). The percent overlap of the LA noon to 6 P.M. sample with the chamber samples was lower than any of the BF data. This difference was likely due to the presence (or the increased concentrations) of other sources in LA, including gasoline SOA which has been asserted to be a dominant source there [Bahreini et al., 2012; P. L. Hayes et al., submitted manuscript, 2012], and/or a

potentially shorter photochemical processing time relative to both BF and the chamber studies.

[18] The bulk H/C, O/C, and N/C elemental ratios are commonly used to characterize SOA, and the corresponding averaged values for all samples, weighted by relative intensities [Bateman *et al.*, 2009; Nguyen *et al.*, 2010], are listed in Table 1. These bulk elemental ratios can be compared with other concurrent measurements obtained using more established methods to support the results from this novel technique. Collocated HR-ToF-AMS were used in both field studies to measure the composition of the aerosol in real time and the uncertainties listed for the AMS data in Table 1 follow those suggested by Aiken *et al.* [2008]. The H/C ratio measured by the nano-DESI method was fairly consistent throughout all of the field and laboratory samples ranging from 1.7 to 1.4 in the LA afternoon (6 P.M. to midnight) and midnight to 6 A.M. samples, respectively. The H/C ratio measured by the AMS was somewhat lower, ranging from 1.3 to 1.5 (Table 1). The O/C ratios measured with the nano-DESI analysis had a slightly larger range with the lowest values measured in the LA samples, between 0.13 and 0.24, and the highest value, 0.46, observed in the ISO-NO_x sample. A comparison of the O/C and N/C values to AMS data must be considered with caution because selective ionization in ESI may lead, depending on the sample and the ionization mode, to either an overestimation or an underestimation of the <O/C> value. In addition, we analyzed only the 0.18–0.32 μm size fraction in the ambient samples which is smaller than the size range sampled by AMS (0.05–1.0 μm). In BF, no dependence of the <O/C> on the aerosol size was found from an analysis of the AMS data so the AMS <O/C> for the ensemble submicron particles is used to represent the <O/C> in the 0.18–0.32 μm size range. The BF <O/C> values of 0.32–0.35 for the positive mode data and 0.56–0.76 for the negative mode data were comparable to the <O/C> values of 0.28–0.44 measured by the AMS on the same day (Tables 1 and S2). Because AMS and nano-DESI-MS employ different ionization techniques, we do not expect a perfect overlap in the bulk elemental ratios between the two data sets. The fact that the majority of the AMS results lie between the results from the two nano-DESI ionization modes suggests that the aerosol elemental compositions measured by both techniques are similar [Bateman *et al.*, 2012]. In contrast, AMS

measurements showed that the <O/C> values in LA were lower and depended on the size of the aerosol (Table S3). The LA data for the nano-DESI-MS analysis had <O/C> values ranging from 0.13 to 0.24 in the positive mode and 0.27–0.63 in the negative mode (Tables 1 and S2). These two ranges bracket the AMS <O/C> values of 0.31–0.39 for the same aerosol size range (Table 1). For the positive mode data, the <N/C> values from BF were about 4 to 14 times higher than average N/C values measured with AMS. In LA, the AMS values were about 0.5 to 9 times higher than the nano-DESI values (Table 1). The AMS N/C values are not size resolved which could explain some, but likely not all, of the differences. More work comparing the responses of the two different techniques to nitrogen containing compounds is necessary to fully understand these observations. The much lower <N/C> values measured in the LA samples with nano-DESI-MS further indicate differences in chemistry between the two sites. Because both the LA and BF regions have plenty of NO_x this difference in the <N/C> is likely indicative of both different aerosol ages and different chemistry leading to nitrogen containing species, as we discuss below.

3.2. Comparing LA to BF

[19] Significant differences were observed in the mass spectral overlap and the <O/C> and <N/C> ratios between the LA and BF samples. The degree of overlap between LA and BF was calculated using equation 2.

$$\% \text{ overlap} = \frac{\text{(number of matching peaks)}}{\text{(number of peaks detected in LA sample)}} \times 100 \quad (2)$$

where “matching peaks” were those identified in both samples. Similar trends were observed with either BF or LA sample placed in the denominator, for brevity only comparisons against LA are discussed. The LA samples with the highest percent overlap with BF data were the two afternoon samples (noon-midnight) and the percent overlap of the four LA samples with each of the BF samples followed a similar pattern as observed in the overlap between LA and the chamber data (Figures 3 and S12). Insights into the differences in SOA composition characteristic for the two locations can be gained from examining the compounds

Table 1. Ensemble Average, Intensity Weighted H/C, O/C, and N/C Values of the Compounds Observed for Each Sample and the AMS Values Averaged Over the Same Sample Time Periods. Only the LA AMS O/C Values are Size Resolved

Sample	Nano-DESI			AMS		
	H/C	O/C	N/C ($\times 10^{-3}$)	H/C	O/C	N/C ($\times 10^{-3}$)
Diesel-NO _x	1.7	0.28	28	-	-	-
Diesel-NO _x -NH ₃	1.6	0.32	39	-	-	-
Isoprene-NO _x	1.7	0.46	44	-	-	-
BF midnight to 6 A.M.	1.6	0.33	42	1.5 ± 0.2	0.28 ± 0.09	3.1 ± 0.7
BF 6 A.M. to noon	1.6	0.32	33	1.4 ± 0.1	0.40 ± 0.1	4.2 ± 0.9
BF noon to 6 P.M.	1.5	0.35	18	1.4 ± 0.1	0.43 ± 0.1	4.1 ± 0.9
BF 6 P.M. to midnight	1.5	0.35	30	1.3 ± 0.1	0.44 ± 0.1	4.6 ± 1
LA midnight to 6 A.M.	1.4	0.19	2.4	1.5 ± 0.2	0.35 ± 0.1	22 ± 5
LA 6 A.M. to noon	1.5	0.13	21	1.4 ± 0.1	0.31 ± 0.1	14 ± 3
LA noon to 6 P.M.	1.7	0.24	19	1.4 ± 0.1	0.39 ± 0.1	6.9 ± 2
LA 6 P.M. to midnight	1.7	0.23	13	1.5 ± 0.2	0.37 ± 0.1	11 ± 2

unique to each sample. The double bond equivalence (DBE), which represents the sum of all rings and double bonds in the molecule, is calculated using equation (3).

$$\text{DBE} = 1 + c - (h/2) + (n/2) \quad (3)$$

where c , h , and n refer to the number of carbon, hydrogen, and nitrogen atoms in the identified species, respectively. This equation assumes a valence of 3 for nitrogen; the calculated DBE will be slightly higher if most of the nitrogen-containing compounds have valence of 5. The percent of unsaturation was calculated by dividing the DBE values for each compound by the number of single bonds in a saturated hydrocarbon with the same number of carbon atoms [Smith *et al.*, 2009]. Figure 4 shows a comparison of the percent unsaturation of the BF and LA noon to 6 P.M. samples which ranged from 0 to around 25% and generally decreased with increasing mass. The unique compounds in BF were more unsaturated (average 11% vs. 8%) and had higher O/C values than the unique compounds in LA. The aromaticity index (AI) [Koch and Dittmar, 2006], an estimation of the number of C=C double bonds, was calculated for the unique BF data to investigate the type of double bonds indicated by the higher unsaturation values in BF. Approximately 62% of the compounds above 200 Da had aromaticity index values of zero, suggesting that many of the double bonds were carbonyls and nitrogen-oxygen functional groups. The higher percent unsaturation for the BF sample in this region is thus largely driven by the increased number of oxygen atoms.

[20] The lower oxidation level of the compounds in LA (Figure 4) suggests this SOA was younger and had undergone less heterogeneous, homogenous, and/or photolytic [Bateman *et al.*, 2011] processing. Since aerosols can grow in size as they age, the observation of younger aerosol in

LA is consistent with the AMS results showing that the average O/C value increased with increasing aerosol size (Table S3). The aerosol sample measured here, in the 0.18–0.32 μm range, was less oxidized than the more processed aerosols found in larger size fractions, although a caveat is that primary aerosols are generally concentrated in the smaller size fractions (P. L. Hayes *et al.*, submitted manuscript, 2012). The compounds with low O/C values unique to the LA samples may also indicate different sources between the two sites.

[21] The younger age of the aerosol can also explain the very low number of nitrogen containing compounds observed in the LA samples despite high NO_x levels. If the aerosol sample in the 0.18–0.32 μm range in LA was only a few hours old then there was less time for organonitrates to form and partition into the particle phase. AMS measurements in LA suggested low concentrations of organonitrates over the whole size range (0.05–1.0 μm) (P. L. Hayes *et al.*, submitted manuscript, 2012). Lower concentrations of organonitrates (PM 2.5) in LA vs. BF were also observed with FTIR analysis. In BF on 23 June, the organonitrate group concentration from FTIR was 0.2 $\mu\text{g}/\text{m}^3$ compared to 0.09 $\mu\text{g}/\text{m}^3$ in LA on 5 June. Thus, the amount of organonitrates was lower overall in LA compared to BF. Also, the much higher nitrogen content in BF could have been driven by the high ammonia levels there (average value of 20 ppb with an hourly maximum of 65 ppb) (M. Z. Markovic *et al.*, manuscript in preparation, 2012), which can result in production of reduced nitrogen compounds [Laskin *et al.*, 2010; Wang *et al.*, 2010].

3.3. Comparing Unique Species Observed in Chamber and Ambient Samples

[22] A comparison of the unique compounds between the chamber experiments can help elucidate their relative contributions to the ambient samples. The hypothesis is that each type of chamber-generated SOA may have a set of unique and reproducible “signature” peaks, which could be used for source apportionment of the field data. An analysis of the overlap between the ISO- NO_x sample (504 total peaks) and the DSL- NO_x sample (732 total peaks) resulted in 401 (55% with respect to the total number of peaks in this sample) unique DSL- NO_x compounds, 173 (34%) unique ISO- NO_x compounds, and 331 compounds that were common to both DSL- NO_x and ISO- NO_x samples. These results demonstrate that there is an overlap in the elemental formulas of the molecules that are formed, after oxidation and oligomerization reactions, from both isoprene and diesel precursors. Approximately 25–30% of the unique DSL- NO_x compounds and approximately 3–5% of the unique ISO- NO_x compounds overlapped (Equation 1) with BF (Figure S14). Since the majority of the overlap between ISO- NO_x and BF consisted of compounds that are common to both ISO- NO_x and DSL- NO_x , we cannot separate the relative contributions of the two sources well. However, given the greater overlap with unique compounds in DSL, it is likely that BF was more influenced by anthropogenic diesel-like sources than by biogenic isoprene-like sources. Part of the difficulty in separating ISO and DSL sources is that many molecular formulas, such as $\text{C}_3\text{H}_4\text{O}_2$ (methylglyoxal), are common to the oxidation of both isoprene and aromatic compounds.

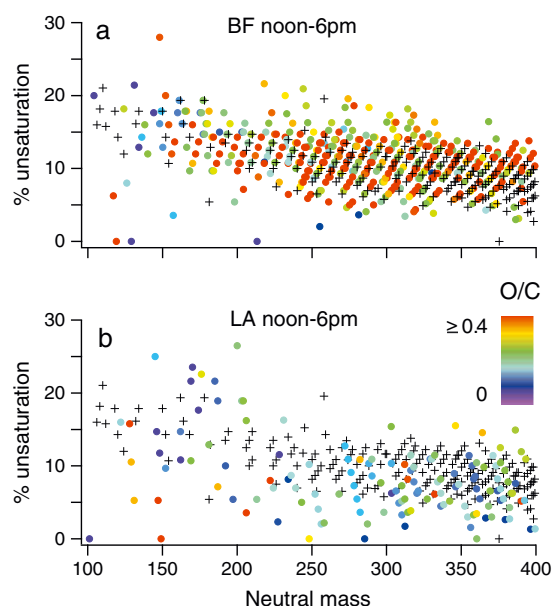


Figure 4. The percent unsaturation of each unique compound plotted vs. the neutral mass for (a) the BF noon to 6 P.M. sample and (b) the LA noon to 6 P.M. sample. The data are color-coded by the O/C value of the compound as indicated in the legend. The grey pluses are the common peaks for comparison.

[23] An analysis of the overlap between the DSL-NO_x-NH₃ sample (595 total peaks) and the DSL-NO_x sample (732 total peaks) resulted in 223 (31%) unique DSL-NO_x compounds and 86 (14%) unique DLS-NO_x-NH₃ compounds. Figure 5 shows the percent overlap (Equation 1) of the BF and LA noon to 6 P.M. samples with the unique DSL-NO_x and unique DSL-NO_x-NH₃. Similar trends in the data were observed for the other samples (Figures S15 and S16). The data are separated by the number of nitrogen atoms in the molecular formulas. In BF, the percent overlap with the unique DSL-NO_x-NH₃ was higher for the 2N compounds, suggesting NH₃-mediated chemistry is responsible for the formation of some of the organic nitrogen in BF. In LA, the percent overlap for the unique DSL-NO_x-NH₃ was slightly higher for 1N compounds than for 0N; however, there was no overlap with the 2N compounds. The unique DSL-NO_x-NH₃ overlap was always lower than the unique DSL-NO_x in LA, suggesting that oxidized nitrogen (e.g., nitric acid esters) played a bigger role in producing SOA in LA than reduced nitrogen (e.g., amines, imines, heterocyclic N-containing compounds). The results obtained from our comparison are consistent with the expectation that urban sites like LA have much lower influence of NH₃ relative to rural/urban sites like BF [Hughes *et al.*, 2000]. Based on other concurrent measurements at the two sites, the mixing ratios of NH₃ in BF were on average ~10 times higher than in LA (M. Z. Markovic *et al.*, manuscript in preparation, 2012; R. A. Ellis *et al.*, Gas-particle partitioning of ammonia at the CalNex-LA ground site and the influence of aerosol pH, *J. Geophys. Res.-Atmos.*, manuscript in preparation, 2012). The higher overlap with the 2N compounds for the unique DSL-NO_x-NH₃ with BF data suggests that some of the 2N compounds observed in BF were formed through reactions of organic compounds with gaseous NH₃ [Laskin *et al.*, 2010; Wang *et al.*, 2010].

4. Conclusions

[24] The molecular composition of aerosol samples collected from chamber studies and in BF and LA during CalNex were investigated using high resolution mass spectrometry. Between 100 and 800 unique compounds were identified in each sample (Figure 2). The percent overlap of the ambient samples with the three chamber experiments each showed

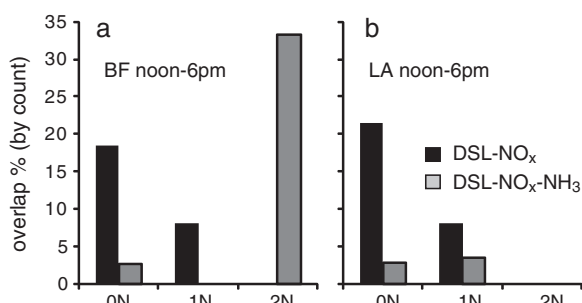


Figure 5. Percent overlap of the unique DSL-NO_x and unique DSL-NO_x-NH₃ peaks with (a) BF noon to 6 P.M. and (b) LA noon to 6 P.M. samples. The data are broken down by the number of nitrogen atoms in the chemical formula. The high overlap between 2N compounds and DSL-NO_x-NH₃ peaks implies an important role of ammonia in forming nitrogen containing compounds in BF.

the same trend: DSL-NO_x had the highest overlap followed by DSL-NO_x-NH₃ and ISO-NO_x (Figure 3). The number of peaks identified for the LA night samples was lower than the number identified for the LA day samples. The highest overlaps with the chamber experiments were observed for the noon-6 P.M. sample, consistent with the SOA plume arriving from downtown LA.

[25] There were significant differences in the mass spectra measured for the LA and BF samples (Figures 1 and S2–S7). A comparison of the molecular compositions in LA and BF showed compounds with higher O/C values and higher percent unsaturation for BF. The higher oxidation level of the BF samples may indicate a fresher LA sample and/or different sources at the two sites. The DSL-NO_x-NH₃ sample had significantly more overlap with the 2N compounds in each BF sample than the DSL-NO_x sample. This suggests that some of the nitrogen containing compounds in BF were formed by NH₃ chemistry. There were significantly more nitrogen containing compounds in the BF samples than in the LA samples consistent with AMS and FTIR results showing low levels of organonitrates in LA. Additionally, the higher number of CHON compounds in BF could have been driven by the higher concentrations of NH₃ in BF.

[26] Combining all the compounds observed in chamber experiments with diesel and isoprene oxidation results in overlap with 70% or less of the ambient compounds. The inherent differences between ambient and chamber experiments, including the increased time for oxidation available in an ambient environment, could explain some of these differences. However, it is evident that diesel and isoprene do not cover the full range of sources contributing to SOA in either BF or LA. The utility of this comparative approach indicates that a more complete assessment of expected sources to the high-MW fraction of the aerosol, including chamber experiments with other SOA precursors such as gasoline [Bahreini *et al.*, 2012; P. L. Hayes *et al.*, submitted manuscript, 2012], terpenes [Pandis *et al.*, 1991; Griffin *et al.*, 1999], and petroleum and cooking emissions [Liu *et al.*, 2012] could be useful in the source apportionment of ambient aerosols.

[27] **Acknowledgments.** The UC Berkeley group acknowledges support from CARB contracts 08-316 and 09-316, and NOAA award NA10OAR4310104. The UCI group acknowledges support by NSF grants ATM-0831518 and CHE-0909227. AL acknowledges support from the Atmospheric System Research program, Office of Biological and Environmental Research (OBER) of the U.S. DOE. The nano-DESI/HR-MS experiments described in this paper were performed at EMSL, a national scientific user facility sponsored by OBER U.S. DOE and located at the Pacific Northwest National Laboratory (PNNL). PNNL is operated for US DOE by Battelle Memorial Institute under Contract No. DE-AC06-76RL01830. SL and LMR acknowledge support from CARB 09-328. We thank Nathan Kreisberg for help with the sampling set-up and John Offenberg and EPA for use of the MOUDI samplers. We thank John Karlik, Ron Cohen, Sally Pusede, University of California Extension Staff, and Kern County Staff, for logistical support in Bakersfield. JJJ and PLH were supported by CARB 08-319/11-305 and by DOE BER/ASR DE-SC0006035. PLH acknowledges a fellowship from the CIRES Visiting Fellows Program.

References

- Aiken, A. C., *et al.* (2008), O/C and OM/OC ratios of primary, secondary, and ambient organic aerosols with high-resolution time-of-flight aerosol mass spectrometry, *Environ. Sci. Technol.*, 42(12), 4478–4485.
- Altieri, K. E., *et al.* (2008), Oligomers formed through in-cloud methylglyoxal reactions: Chemical composition, properties, and mechanisms investigated by ultra-high resolution FT-ICR mass spectrometry, *Atmos. Environ.*, 42(7), 1476–1490.

- Altieri, K. E., B. J. Turpin and S. P. Seitzinger (2009), Oligomers, organosulfates, and nitrooxy organosulfates in rainwater identified by ultra-high resolution electrospray ionization FT-ICR mass spectrometry, *Atmos. Chem. Phys.*, *9*(7), 2533–2542.
- Bahreini, R., et al. (2012), Gasoline emissions dominate over diesel in formation of secondary organic aerosol mass, *Geophys. Res. Lett.*, *39* (6), L06805.
- Baltensperger, U., et al. (2005), Secondary organic aerosols from anthropogenic and biogenic precursors, *Faraday Discuss.*, *130*, 265–278.
- Bateman, A. P., et al. (2008), The effect of solvent on the analysis of secondary organic aerosol using electrospray ionization mass spectrometry, *Environ. Sci. Technol.*, *42*(19), 7341–7346.
- Bateman, A. P., J. Laskin, A. Laskin, and S. Nizkorodov (2012), Applications of high-resolution electrospray ionization mass spectrometry to measurements of average oxygen to carbon ratios in secondary organic aerosols, *Environ. Sci. Technol.*, *46*, 8315–8324.
- Bateman, A. P., S. A. Nizkorodov, J. Laskin, and A. Laskin (2009), Time-resolved molecular characterization of limonene/ozone aerosol using high-resolution electrospray ionization mass spectrometry, *Phys. Chem. Chem. Phys.*, *11*(36), 7931–7942.
- Bateman, A. P., S. A. Nizkorodov, J. Laskin, and A. Laskin (2011), Photolytic processing of secondary organic aerosols dissolved in cloud droplets, *Phys. Chem. Chem. Phys.*, *13*(26), 12199–12212.
- Carlton, A. G., C. Wiedinmyer, and J. H. Kroll (2009), A review of secondary organic aerosol (SOA) formation from isoprene, *Atmos. Chem. Phys.*, *9*, 4987–5005.
- Charlson, R. J., et al. (1992), Climate Forcing by Anthropogenic Aerosols, *Science*, *255*(5043), 423–430.
- DeCarlo, P. F., et al. (2004), Particle morphology and density characterization by combined mobility and aerodynamic diameter measurements. Part 1: Theory, *Aerosol Sci. Technol.*, *38*(12), 1185–1205.
- DeCarlo, P. F., et al. (2006), Field-deployable, high-resolution, time-of-flight aerosol mass spectrometer, *Anal. Chem.*, *78*(24), 8281–8289.
- Dommen, J., et al. (2006), Laboratory observation of oligomers in the aerosol from isoprene/NO(x) photooxidation, *Geophys. Res. Lett.*, *33* (13), L13805, 10.1029/2006GL026523.
- Donahue, N. M., A. L. Robinson, and S. N. Pandis (2009), Atmospheric organic particulate matter: From smoke to secondary organic aerosol, *Atmos. Environ.*, *43*(1), 94–106.
- Eckert, P. A., P. J. Roach, A. Laskin, and J. Laskin (2012), Chemical Characterization of Crude Petroleum Using Nanospray Desorption Electrospray Ionization Coupled with High-Resolution Mass Spectrometry, *Anal. Chem.*, *84*(3), 1517–1525.
- Ervens, B., B. J. Turpin, and R. J. Weber (2011), Secondary organic aerosol formation in cloud droplets and aqueous particles (aqSOA): a review of laboratory, field and model studies, *Atmos. Chem. Phys.*, *11*(21), 11069–11102.
- Fenn, J. B., et al. (1990), Electrospray Ionization-Principles and Practice, *Mass Spectrom. Rev.*, *9*(1), 37–70.
- Gao, S., et al. (2004), Particle phase acidity and oligomer formation in secondary organic aerosol, *Environ. Sci. Technol.*, *38*(24), 6582–6589.
- Goldstein, A. H., and I. E. Galbally (2007), Known and unexplored organic constituents in the earth's atmosphere, *Environ. Sci. Technol.*, *41*(5), 1514–1521.
- Griffin, R. J., D. R. Cocker, R. C. Flagan, and J. H. Seinfeld (1999), Organic aerosol formation from the oxidation of biogenic hydrocarbons, *J. Geophys. Res.-Atmos.*, *104*(D3), 3555–3567.
- Hall, W. A., and M. V. Johnston (2011), Oligomer Content of alpha-Pinene Secondary Organic Aerosol, *Aerosol Sci. Technol.*, *45*(1), 37–45.
- Hughes, L. S., et al. (2000), Evolution of atmospheric particles along trajectories crossing the Los Angeles basin, *Environ. Sci. Technol.*, *34*(15), 3058–3068.
- Iinuma, Y., O. Boge, T. Gnauk, and H. Herrmann (2004), Aerosol-chamber study of the alpha-pinene/O₃ reaction: influence of particle acidity on aerosol yields and products, *Atmos. Environ.*, *38*(5), 761–773.
- Jaitly, M., et al. (2009), Decon2LS: An open-source software package for automated processing and visualization of high resolution mass spectrometry data, *BMC Bioinformatics*, *10*, 87.
- Kalberer, M., et al. (2004), Identification of polymers as major components of atmospheric organic aerosols, *Science*, *303*(5664), 1659–1662.
- Kalberer, M., M. Sax, and V. Samburova (2006), Molecular size evolution of oligomers in organic aerosols collected in urban atmospheres and generated in a smog chamber, *Environ. Sci. Technol.*, *40*(19), 5917–5922.
- Kanakidou, M., et al. (2005), Organic aerosol and global climate modelling: a review, *Atmos. Chem. Phys.*, *5*, 1053–1123.
- Kendrick, E. (1963), A Mass Scale Based on Ch₂=14.0000 for High Resolution Mass Spectrometry of Organic Compounds, *Anal. Chem.*, *35* (13), 2146–2154.
- Koch, B. P., and T. Dittmar (2006), From mass to structure: an aromaticity index for high-resolution mass data of natural organic matter, *Rapid Commun. Mass Spectrom.*, *20*(5), 926–932.
- Laskin, A. et al. (2012), Mass spectrometric approaches for chemical characterization of atmospheric aerosols: critical review of the most recent advances, *Environ. Chem.*, *9*, 163–189.
- Laskin, J., et al. (2010), High-Resolution Desorption Electrospray Ionization Mass Spectrometry for Chemical Characterization of Organic Aerosols, *Anal. Chem.*, *82*(5), 2048–2058.
- Lin, P., A. G. Rincon, M. Kalberer, and J. Z. Yu (2012), Elemental Composition of HULIS in the Pearl River Delta Region, China: Results Inferred from Positive and Negative Electrospray High Resolution Mass Spectrometric Data, *Environ. Sci. Technol.*, *46*(14), 7454–7462.
- Liu, S., D. A. Day, J. E. Shields, and L. M. Russell (2011), Ozone-driven daytime formation of secondary organic aerosol containing carboxylic acid groups and alkane groups, *Atmos. Chem. Phys.*, *11* (16), 8321–8341.
- Liu, S., et al. (2012), Secondary organic aerosol formation from fossil fuel sources contribute majority of summertime organic mass at Bakersfield, *J. Geophys. Res.-Atmos.*, *117*, D00V26, doi:10.29192/JD018170.
- Marshall, A. G., K. Sunghwan and R. P. Rodgers (2006), Truly "exact" mass: Elemental composition can be determined uniquely from molecular mass measurement at ~0.1mDa accuracy for molecules up to ~500 Da, *Int. J. Mass Spectrom. (Netherlands)*, *251*(2-3), 260–265.
- Mazzoleni, L. R., et al. (2010), Water-Soluble Atmospheric Organic Matter in Fog: Exact Masses and Chemical Formula Identification by Ultrahigh-Resolution Fourier Transform Ion Cyclotron Resonance Mass Spectrometry, *Environ. Sci. Technol.*, *44*(10), 3690–3697.
- Nguyen, T. B., et al. (2010), High-resolution mass spectrometry analysis of secondary organic aerosol generated by ozonolysis of isoprene, *Atmos. Environ.*, *44*(8), 1032–1042.
- Nguyen, T. B., J. Laskin, A. Laskin, and S. A. Nizkorodov (2011a), Nitrogen-Containing Organic Compounds and Oligomers in Secondary Organic Aerosol Formed by Photooxidation of Isoprene, *Environ. Sci. Technol.*, *45*(16), 6908–6918.
- Nguyen, T. B., et al. (2011b), Effect of humidity on the composition of isoprene photooxidation secondary organic aerosol, *Atmos. Chem. Phys.*, *11*(14), 6931–6944.
- Nizkorodov, S. A., J. Laskin, and A. Laskin (2011), Molecular chemistry of organic aerosols through the application of high resolution mass spectrometry, *Phys. Chem. Chem. Phys.*, *13*(9), 3612–3629.
- NOAA: National Oceanic and Atmospheric Administration (2008), 2010 CalNex White Paper: Research at the Nexus of Air Quality and Climate Change, Available at: <http://www.esrl.noaa.gov/csd/projects/calnex/whitepaper.pdf>.
- Pandis, S. N., S. E. Paulson, J. H. Seinfeld, and R. C. Flagan (1991), Aerosol Formation in the Photooxidation of Isoprene and Beta-Pinene, *Atmos. Environ. Part A*, *25*(5-6), 997–1008.
- Pope, C. A., and D. W. Dockery (2006), Health effects of fine particulate air pollution: Lines that connect, *J. Air Waste Manage. Assoc.*, *56*(6), 709–742.
- Reemtsma, T., et al. (2006), Identification of fulvic acids and sulfated and nitrated analogues in atmospheric aerosol by electrospray ionization Fourier transform ion cyclotron resonance mass spectrometry, *Anal. Chem.*, *78*(24), 8299–8304.
- Reinhardt, A., et al. (2007), Ultrahigh mass resolution and accurate mass measurements as a tool to characterize oligomers in secondary organic aerosols, *Anal. Chem.*, *79*(11), 4074–4082.
- Roach, P. J., J. Laskin, and A. Laskin (2010a), Molecular Characterization of Organic Aerosols Using Nanospray-Desorption/Electrospray Ionization-Mass Spectrometry, *Anal. Chem.*, *82*(19), 7979–7986.
- Roach, P. J., J. Laskin, and A. Laskin (2010b), Nanospray desorption electrospray ionization: an ambient method for liquid-extraction surface sampling in mass spectrometry, *Analyst*, *135*(9), 2233–2236.
- Roach, P. J., J. Laskin, and A. Laskin (2011), Higher-Order Mass Defect Analysis for Mass Spectra of Complex Organic Mixtures, *Anal. Chem.*, *83*(12), 4924–4929.
- Rudich, Y., N. M. Donahue, and T. F. Mentel (2007), Aging of organic aerosol: Bridging the gap between laboratory and field studies, *Annu. Rev. Phys. Chem.*, *58*, 321–352.
- Russell, L. M., et al. (2009), Oxygenated fraction and mass of organic aerosol from direct emission and atmospheric processing measured on the R/V Ronald Brown during TEXAQS/GoMACCS 2006, *J. Geophys. Res.-Atmos.*, *114*, D00F05, doi:10.1029/2008JD011275.
- Schmitt-Kopplin, P., et al. (2010), Analysis of the Unresolved Organic Fraction in Atmospheric Aerosols with Ultrahigh-Resolution Mass Spectrometry and Nuclear Magnetic Resonance Spectroscopy: Organosulfates As Photochemical Smog Constituents, *Anal. Chem.*, *82*(19), 8017–8026.
- Seinfeld, J. H., and J. F. Pankow (2003), Organic atmospheric particulate material, *Annu. Rev. Phys. Chem.*, *54*, 121–140.
- Smith, J. S., A. Laskin, and J. Laskin (2009), Molecular Characterization of Biomass Burning Aerosols Using High-Resolution Mass Spectrometry, *Anal. Chem.*, *81*(4), 1512–1521.
- Stenson, A. C., A. G. Marshall, and W. T. Cooper (2003), Exact masses and chemical formulas of individual Suwannee River fulvic acids from ultrahigh resolution electrospray ionization Fourier transform ion cyclotron resonance mass spectra, *Anal. Chem.*, *75*(6), 1275–1284.

- Tolocka, M. P., et al. (2004), Formation of oligomers in secondary organic aerosol, *Environ. Sci. Technol.*, *38*(5), 1428–1434.
- Walser, M. L., et al. (2008), High-resolution mass spectrometric analysis of secondary organic aerosol produced by ozonation of limonene, *Phys. Chem. Chem. Phys.*, *10*(7), 1009–1022.
- Wang, X. F., et al. (2010), Evidence for High Molecular Weight Nitrogen-Containing Organic Salts in Urban Aerosols, *Environ. Sci. Technol.*, *44*(12), 4441–4446.
- Weitkamp, E. A., et al. (2007), Organic aerosol formation from photochemical oxidation of diesel exhaust in a smog chamber, *Environ. Sci. Technol.*, *41*(20), 6969–6975.
- Williams, B. J., et al. (2010), Major components of atmospheric organic aerosol in southern California as determined by hourly measurements of source marker compounds, *Atmos. Chem. Phys.*, *10*(23), 11577–11603.
- Wilson, J. L., et al. (1990), Laboratory Investigation of Residual Liquid Organics In United States Environmental Protection Agency: 1990; Vol. EPA 600/6-90/004.
- Zhang, H., et al. (2011), Effect of relative humidity on SOA formation from isoprene/NO photooxidation: enhancement of 2-methylglyceric acid and its corresponding oligoesters under dry conditions, *Atmos. Chem. Phys.*, *11*(13), 6411–6424.
- Zhang, Q., et al. (2005), Time- and size-resolved chemical composition of submicron particles in Pittsburgh: Implications for aerosol sources and processes, *J. Geophys. Res.-Atmos.*, *110*, D07S09, doi: 10.1029/2004JD004649.
- Zhang, Q., et al. (2007), Ubiquity and dominance of oxygenated species in organic aerosols in anthropogenically-influenced Northern Hemisphere midlatitudes, *Geophys. Res. Lett.*, *34*, L13801, doi:10.1029/2007GL029979.